Project Description

Scientific Rationale

The character of deep convection and the means by which it is forced are of supreme importance to all tropical circulations, including tropical cyclones, tropical waves, the Madden-Julian oscillation, the ITCZ, and the Hadley and Walker cells. The purpose of this proposal is to make the measurements in the east Pacific and southwest Caribbean that are needed to understand how convection there works together with the large scale circulations in this region.

Convection in the east Pacific and southwest Caribbean differs from that in previously studied areas of the western Atlantic and Pacific in that sea surface temperatures (SSTs) are lower and boundary layer forcing is stronger. Convection forms in different circumstances in the east Pacific and in the southwest Caribbean; in the former, strong SST gradients drive potent forcing, whereas in the latter, convection forms where these gradients are weak and the mid-troposphere is often very dry. However, upstream orographic forcing from Central America may be operating there. Forms of convection exist in the east Pacific intertropical convergence zone (ITCZ) that until recently were not recognized in satellite-based estimates of precipitation and convective vertical structure.

Tropical easterly waves and related phenomena are ubiquitous in the tropical regions of the world. Aside from being significant weather makers in their own right, such waves are frequent precursors to tropical cyclones. East Pacific waves appear to result either from African waves that reintensify in the far east Pacific or else they form there. This formation or reintensification appears to result from a combination of barotropic and convective energy conversions. The latter depends sensitively on the vertical structure of the convection, which brings us back to the issues raised above. The way convection interacts with easterly waves is likely to be characteristic of this interaction for many types of tropical disturbances.

Prior Field Campaigns

EPIC2001 and ECAC

EPIC2001 (East Pacific Investigation of Climate; Raymond et al., 2004), based in Huatulco, México in the late summer and early fall of 2001, painted a detailed picture of the mean state of the east Pacific ITCZ. This picture was derived from dropsondes deployed by the NCAR C-130 aircraft in 8 flights along 95 W between 12 N and the equator (see figure 1, left panel).

The east Pacific is characterized by a strong, cross-equatorial SST gradient, as figure 1 shows. This drives a southeasterly boundary layer flow which veers to southwesterly as it moves into the northern hemisphere. The flow terminates in a narrow east-west convergence zone that defines the east Pacific ITCZ. The latitude of this convergence zone varies significantly from day to day, resulting in latitudinal smearing of the convergence between 4 N and 12 N on the average, as indicated by the nearly linear decrease in the mean meridional wind over this latitude range in the top plot in the left panel of figure 2. Notice that the ITCZ does not occur at the SST maximum, which is located near the Mexican coast.

The existence of deep convection in or near the ITCZ is highly variable and is associated with the passage of easterly waves, as figure 1 right panel shows. When it is present, there is a deep, cross-equatorial Hadley circulation, with the northerly return flow occurring in the upper troposphere. In the absence of deep convection, a shallow Hadley circulation exists with the return flow occurring near 850 hPa (Zhang et al., 2004).

Balanced models of boundary layer flows driven by SST gradients (Zebiak, 1982, 1986; Lindzen and Nigam, 1987; Battisti et al., 1999; Stevens et al., 2002; McGauley et al., 2004; Back and
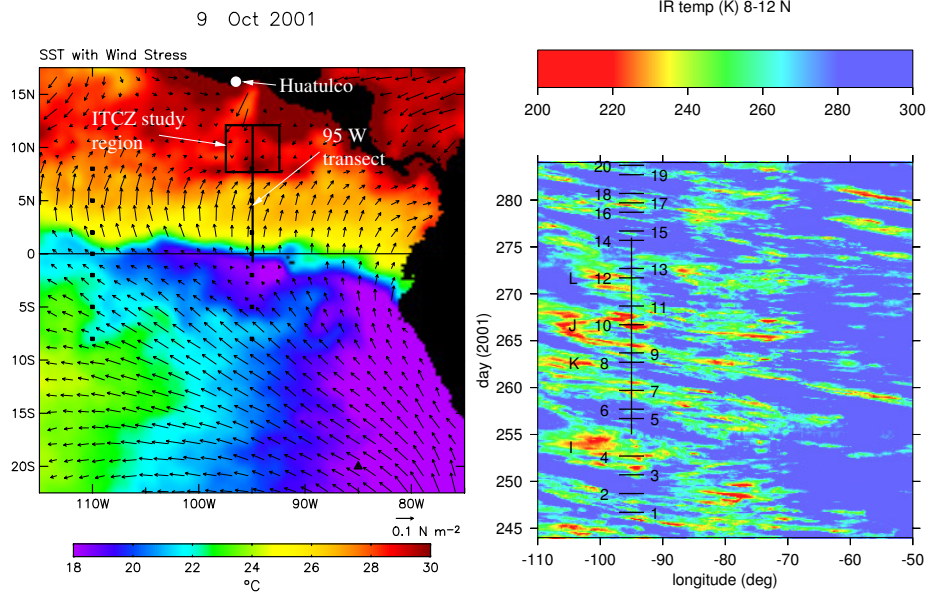
Figure 1: Left panel: Sea surface temperature and surface wind stress on 9 October 2001. Shown also are the 95 W transect of the C-130 and the ITCZ study region. Right panel: Infrared brightness temperature as a function of longitude and time during EPIC2001, averaged over $8 - 12$ N. Both taken from Raymond et al. (2004).

Bretherton, 2009a,b) have been used to explain the observed structure of boundary layer convergence in the tropics. These models derive the boundary layer winds from an Ekman balance condition with the possible addition of eddy transport of momentum into the boundary layer from above.

Figure 2, left panel, upper plot, shows that Ekman balance theories do a reasonable job explaining the average meridional flow in the planetary boundary layer. However, as the middle plot indicates, the standard deviation of the meridional wind in the 8 cases grows in magnitude north of 7 N to quite substantial values. As Raymond et al. (2006) show, Ekman balance on days with strong deep convection tends to fail badly, whereas the theory fares much better when there is little or no deep convection.

Another curious feature of deep convection in the east Pacific is that the infrared brightness temperature shows a sharp minimum at 8 N (Raymond et al., 2006; see figure 5) in spite of the fact that boundary layer convergence on the average is uniformly distributed from 4 N to 12 N. This calls into question the existence of a direct relationship between boundary layer convergence and deep convection in this region.

Raymond et al. (2003) found a strong inverse relationship between surface moist entropy flux and infrared brightness temperature during EPIC2001. This is in agreement with the boundary layer quasi-equilibrium theory of Raymond (1995), in which there is a balance primarily between surface fluxes, which tend to increase the moist entropy of the boundary layer and downdraft fluxes, which tend to decrease it. Since downdrafts scale with updrafts in convection (with a possibly variable coefficient), surface moist entropy fluxes should therefore be instrumental in driving deep convection. Figure 2, right panel, shows that this appears to have been true during EPIC2001; the positive entropy tendency due to surface moist entropy fluxes is highly correlated with infrared brightness temperature, whereas the horizontal entropy convergence associated with mass convergence in the ITCZ is not. Using modeling and buoy plus satellite observations, Maloney and Esbensen (2005,
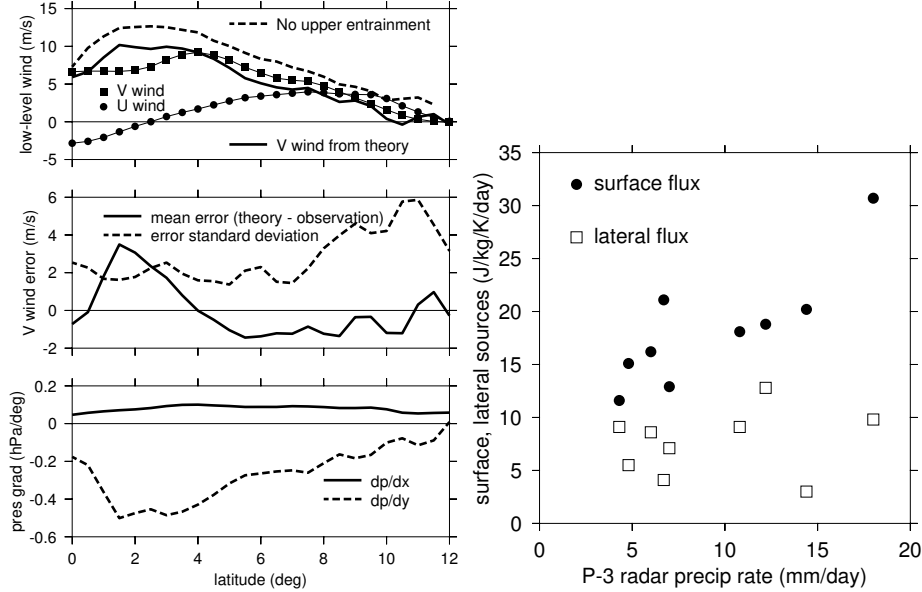
Figure 2: Left panel: Average of 8 C-130 flights in EPIC2001. Top plot: Zonal and meridional winds in planetary boundary layer along 95 W along with results of an Ekman balance model with and without momentum entrainment from above. Middle plot: Mean and standard deviation of the meridional wind error. Bottom plot: Zonal and meridional pressure gradients in the planetary boundary layer. Right panel: Entropy tendencies in the planetary boundary layer as a function of precipitation rate in the ITCZ study region from 9 P-3 flights. Solid dots show the tendencies from surface heat fluxes while squares show those from lateral entropy convergence. Both plots taken from Raymond et al. (2006).

2007) also concluded that deep convection was highly correlated with surface heat fluxes. This is further evidence that the Ekman-driven convergence in the east Pacific boundary layer has at best an indirect relationship to deep convection there.

During ECAC (Experimento Climático en las Albercas de Agua Cálida; Amador, 2008), the Mexican oceanographic research vessel *Justo Serra* deployed radiosondes in the southwest Caribbean region. Figure 3 shows the moist entropy, saturated moist entropy, and the wind speed from a sounding deployed in the core of the southwest Caribbean low-level jet during a particularly active phase. The sounding shows a reasonably well mixed planetary boundary layer below 900 hPa topped by a strong inversion and extremely dry free tropospheric air. The wind speed profile shows an ENE jet with 16 m s^{-1} winds at the surface and wind speeds in excess of 20 m s^{-1} near 850 hPa, yet no deep convection formed. Satellite observations show on the average that deep convection only develops as this jet approaches the Central American coast (Zuluaga and Houze, 2015) in spite of uniformly warm ocean waters.

The Caribbean offshore from Central America is not always so convectively benign. For instance, the right panel of figure 1 shows that the precursor to Hurricane Juliette (2001) was continuously visible in the infrared through the southwest Caribbean, and in fact was tracked in real time from its origin in Africa during the EPIC2001 project. Thus, significant deep convection can exist there. However it appears that starting such convection where none exists previously is very difficult, even in the presence of strong surface heat fluxes. This may be a case of multiple convective equilibria (Sobel et al., 2007; Sessions et al., 2010).

EPIC2001 and ECAC taught us a great deal about the eastern Pacific and the southwest
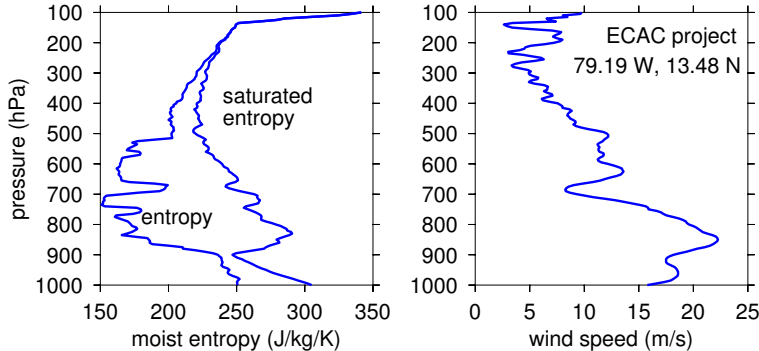
Figure 3: Sounding from the ECAC project on 17 July 2001 near 79.19 W, 13.48 N or about 450 km north of Panama City in the southwest Caribbean. Data courtesy of Victor Magaña.

Caribbean. However, given the facilities available to us at the time, they were unable to address key questions about the form of convection there and its interaction with the large scale.

TPARC/TCS08 and PREDICT

The THORPEX Pacific Asian Regional Campaign/Tropical Cyclone Structure (TPARC/TCS08) and the Pre-Depression Investigation of Cloud-Systems in the Tropics (PREDICT) field programs used grids of dropsondes deployed from high altitude as well as airborne Doppler radar (TPARC/TCS08 only) to investigate tropical convection associated with potential tropical cyclone precursor systems.

Based on a three-dimensional variational analysis scheme developed by López and Raymond (2011), Raymond and López (2011), Raymond et al. (2011), and Gjorgjievska and Raymond (2014) used this technology to diagnose the mass, vorticity and thermodynamic budgets of convection in potentially developing cyclones, relating them to the characteristics of the environment in which the convection was embedded.

These results are summarized by Raymond et al. (2014), from which figure 4 is borrowed. The saturation fraction is the precipitable water in a column divided by the saturated precipitable water and is thus a column relative humidity.

The instability index is the difference between the $1 - 3$ km and $5 - 7$ km saturated specific moist entropy values. It is a measure of the deviation of the actual temperature profile from a moist adiabat in the lower free troposphere and therefore indicates low to mid-tropospheric moist convective (not conditional) instability; if the thermodynamic profile is moist-neutral, then the instability index is zero. Instability index is related to the lower tropospheric convective available potential energy, but it is not exactly the same, as the lifted parcel starts from the $1 - 3$ km layer and is assumed to be initially saturated.

The upper left plot in figure 4 shows that saturation fraction and instability index are strongly anti-correlated, at least in regions of active convection. This is likely the expression of "moisture quasi-equilibrium", a process explored by Singh and O'Gorman (2013). In this process convection actually adjusts the surrounding humidity to maintain nearly neutral parcel buoyancy for an entraining parcel. This occurs because negative buoyancy caused by mixing of cloud with dry air results in convective detrainment, which moistens the column, whereas large positive buoyancy in a moist local environment results in strong upward acceleration of ascending parcels, which by mass continuity draws in dry surrounding air, resulting in drying of the column. These feedbacks drive the humidity toward an equilibrium value in which actual convective parcels maintain near-neutral

4

buoyancy. Since greater undilute parcel buoyancy allows parcels to withstand the entrainment of drier air while still remaining buoyant, the equilibrium humidity depends inversely on moist convective instability, and hence the instability index.

The existence of moisture quasi-equilibrium suggests that the saturation fraction is not a predictor of precipitation, but rather a co-variant, at least on time scales longer than that required to produce moisture quasi-equilibrium. Establishment of moisture quasi-equilibrium was explored by Raymond (2000) and was found to proceed at a much more rapid pace when the atmosphere is already moist and strongly convective.

When moisture quasi-equilibrium holds, the instability index becomes a predictor variable for both saturation fraction and precipitation. The question then becomes, what controls the instability index? This index is purely a function of the temperature profile, which according to the weak temperature gradient approximation should be nearly uniform in the tropics (Sobel and Bretherton, 2000). Thus, variations of the instability index must be sought in secondary effects, preeminently the small variations in temperature associated with the balanced response to the vorticity distribution.

The theory of such temperature perturbations and their effects on convection are summarized in Raymond et al. (2014) and Raymond et al. (2015). The upshot of a great deal of observational and modeling work for tropical conditions is that the thermal response to a strong, convectively generated mid-level vortex is sufficient to have major effects on the instability index. This occurs by virtue of the balanced generation of a warm anomaly above the vortex and a cool anomaly below, which decreases this index. (This result may be understood from the point of view of potential vorticity inversion. Alternatively, consider the thermal wind effect associated with change in the vortical circulation with height above and below the vorticity maximum.) Indeed, the lower left plot of figure 4 shows that the instability index decreases strongly as the strength of a mid-level vortex increases.

The concept of gross moist stability is central to understanding the effect of variations in instability index. The normalized gross moist stability (NGMS; Raymond et al., 2009) is defined as the vertically integrated lateral export of moist entropy divided by the integrated lateral import of moisture into a column, normalized to be dimensionless. In the steady state this reduces to

$$\gamma = \frac{T_R(E_S - E_T)}{L(P - R_S)} \tag{1}$$

where E_S and E_T are the surface and tropopause fluxes of moist entropy, R_S is the surface evaporation rate, and P is the precipitation rate (Raymond et al. 2009). The constants T_R and L are a constant reference temperature and the latent heat of evaporation. Solving this equation for the precipitation yields

$$P = R_S + \frac{T_R(E_S - E_T)}{L\gamma}. \tag{2}$$

We refer to $E_S - E_T$ as the entropy forcing. Thus, the net rainfall rate $P - R_s$ is proportional to the ratio of the entropy forcing to the NGMS.

The NGMS is predictable from environmental conditions. The upper right plot of figure 4 shows that the NGMS is positively correlated with the instability index, and hence negatively correlated with the strength of the mid-level vorticity. Mid-level vortices can be produced by convection with top-heavy mass flux profiles, i.e., with maximum vertical mass flux in the upper troposphere, which then have strong effects on subsequent convection. In particular, the smaller instability index associated with the mid-level vortex results in more bottom-heavy mass flux profiles (see Raymond and Sessions, 2007; Raymond et al., 2014; Sessions et al., 2015), which produces smaller
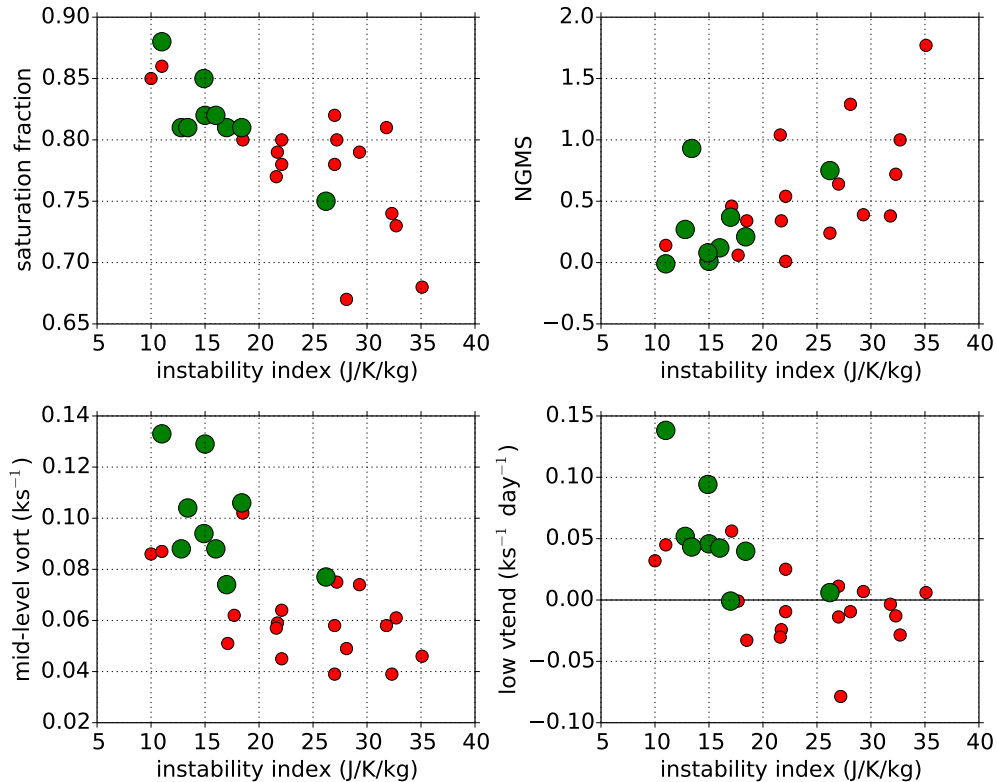
Figure 4: Scatter plots of results from TPARC/TCS08 and PREDICT case studies. The large green dots indicate systems that intensified into tropical storms within 48 hr. Taken from Raymond et al. (2014).

NGMS because the main lateral inflow is from boundary layer air which has higher values of moist entropy than the mid-level air drawn in by convection with top-heavy mass flux profiles. Thus, the combination of mid-level vorticity and strong surface entropy fluxes produces strong rainfall:

$$
\begin{aligned}
\text{top-heavy convection} \quad & \Rightarrow \quad \text{strong mid-level vorticity} \\
& \Rightarrow \quad \text{small instability index} \\
& \Rightarrow \quad \text{bottom-heavy convection} \\
& \Rightarrow \quad \text{low NGMS} \qquad\qquad\qquad\qquad (3)
\end{aligned}
$$

$$
\text{low NGMS + strong surface entropy flux} \Rightarrow \text{high humidity and heavy rain} \qquad (4)
$$

Bottom-heavy mass flux profiles have the additional effect of spinning up low-level vorticity, leading to possible tropical cyclogenesis. The lower right panel of figure 4 illustrates this process in our sample of case studies. Note that the cases of tropical storm formation within 48 hr in this sample (large green dots) are indeed correlated with smaller instability index, lower NGMS, and stronger mid-level vorticity.

We emphasize that the role of vorticity here is completely different than that in mid-latitude quasi-geostrophic dynamics, in which ascending motion is manifested mostly as flows up tilted

isentropic surfaces. In contrast, vorticity in the tropics appears to act by altering the temperature profile, which in turn changes the instability index, and hence the form of the convection.

Scientific Issues and Hypotheses

Convective Initiation

Initial development of deep convection occurs in two regions, in the northward flow of planetary boundary layer air south of the east Pacific ITCZ and in the southwest Caribbean jet as it approaches the Central American coast. These two regions are very different. In the east Pacific, the planetary boundary layer gains energy as it moves northward across increasing SSTs. Furthermore, the free troposphere isn't particularly dry, receiving southward-moving moisture detrained from deep convection further north. It is easy to imagine convection beginning when the boundary layer becomes warm and moist enough for convective inhibition to decrease (as seen in figure 5) and for convective available potential energy to turn positive. However, convective initiation has not been well studied even in this relatively simple case.

In contrast, convective development in the southwest Caribbean is much more of a mystery. The sea surface is warm and the SST distribution is relatively flat. The air aloft can be very dry, as figure 3 shows. Yet, as Zuluaga and Houze (2015) indicate, deep convection develops as this jet approaches Costa Rica and Nicaragua. Perhaps the topography of Central America is exerting upstream influence, much as occurs as the Tradewinds approach the Island of Hawaii (Smolarkiewicz et al., 1988). However, unlike Hawaii, convection develops well into the dry tropospheric air near Central America. The competition between updrafts moistening the air and evaporative and radiative cooling generating subsidence needs to be understood.

The southwest Caribbean is also affected occasionally by pre-existing easterly waves and tropical cyclones, which seem capable of maintaining their convective activity in a dry environment if they are sufficiently strong. This may be a case in which multiple convective equilibria exist (Sobel et al., 2007; Sessions et al., 2010). Strong radiative cooling in the planetary boundary layer appears to be central to the existence of multiple equilibria (Sessions et al., 2015).

The southwest Caribbean is a prototype for other areas with similar physics such as the Somali jet (e.g., Halpern and Woiceshyn, 2001) of the western Indian Ocean. In general, such regions have not been subject to intensive in situ observations. More needs to be learned about how pre-existing dry air suppresses convection and how this suppression is overcome.

Convective Structure and Amount

Insight derived from the tropical cyclogenesis field programs TPARC/TCS08 and PREDICT suggests that we should examine the instability index of the east Pacific environment in the 95 W transect discussed above. Figure 5 shows the infrared brightness temperature, the deep convective inhibition (DCIN = saturated entropy in the $810 - 830$ hPa layer minus the moist entropy in the $900 - 1000$ hPa layer), the saturation fraction, and the instability index (slightly modified to account for the flight level of the aircraft) as a function of latitude along 95 W, as derived from EPIC2001 observations (Raymond et al., 2003, 2006).

South of some point (roughly 6 N on the average), the DCIN is large enough to preclude deep convection. North of this latitude the instability index increases monotonically from about 8 J kg^{-1} K^{-1} to 20 J kg^{-1} K^{-1}. Results from the tropical cyclogenesis programs suggest therefore that humidity and rainfall should *decrease* northward from a maximum slightly to the north of 6 N as instability index increases. As figure 5 indicates, the observed infrared brightness temperature and saturation fraction reflect this pattern with a small deviation near 12 N.
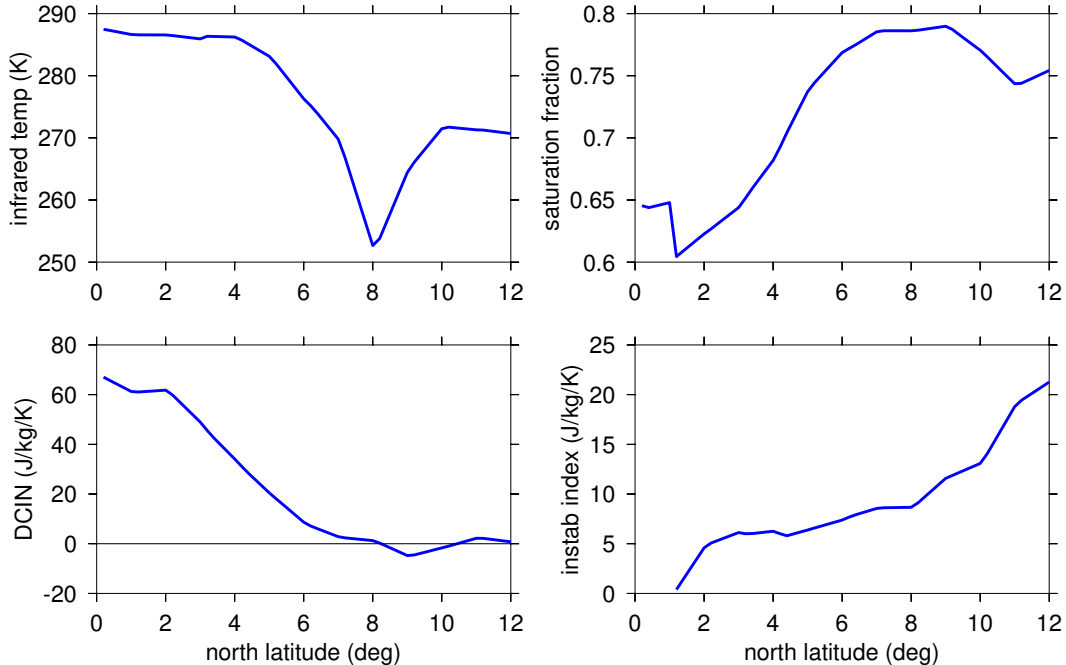
7

Figure 5: Plots derived from the 95 W transects made during EPIC2001. Upper left: Infrared brightness temperature. Lower left: Deep convective inhibition. Upper right: Saturation fraction. Lower right: Instability index.

Deep convection also shows a strong positive dependence on surface moist entropy fluxes as indicated in figure 2. These two results suggest that convection in the tropical east Pacific behaves much as it does elsewhere in the tropics (e.g., Raymond, 1995; Maloney and Sobel, 2004; Maloney and Esbensen, 2005, 2007; Sobel et al., 2009) in spite of the strong SST gradient in the east Pacific. The results also suggest that convective mass fluxes in the east Pacific progress from bottom-heavy toward top-heavy with increasing latitude.

Back and Bretherton (2009a,b) present an alternative point of view of convective forcing in which tropical deep convection consists of two components with top-heavy and bottom-heavy mass flux profiles respectively. The top-heavy component is driven by conditional instability whereas the bottom-heavy part is driven by convergence in the planetary boundary layer. This convergence is predicted by a slab boundary layer model based on Ekman balance (e.g., Zebiak, 1982; Lindzen and Nigam, 1987; Chiang and Zebiak, 2000) plus downward transport of momentum from the free troposphere (Stevens et al., 2002; McGauley et al., 2004). The convection in the east Pacific ITCZ is asserted to be driven mostly by planetary boundary layer convergence associated with the SST gradient, which gives it a bottom-heavy mass flux profile. We thus have two very different hypotheses regarding the environmental control of convection in the east Pacific.

To complicate matters further, there are conflicting hypotheses about the the form of convective mass flux profiles in the east Pacific, with TRMM precipitation radar products suggesting that east Pacific convection is top-heavy (Schumacher et al., 2004) whereas various global analysis products show bottom-heavy profiles (Handlos and Back, 2014). Top-heaviness in the TRMM precipitation algorithm is associated with a large stratiform rain fraction, which in turn comes from, among other criteria, the existence of widespread bright band echo structure, indicating the melting of ice crystal aggregates at the freezing level (Schumacher and Houze, 2003). Based on an improved algorithm and inspection of individual cases, Houze et al. (2015) concluded that certain types of

rainfall registering as "stratiform" are actually due to "weak cellular convection" which produces bright bands and exhibits vertical mass flux profiles that are not top heavy. However, we still lack actual measurements of mass flux profiles in this case.

The importance of vertical mass flux profiles is that they are directly related to convective heating profiles. As Hartmann et al. (1984), Schumacher et al. (2004), and many others have indicated, large-scale circulations in the tropics are highly sensitive to variations in these profiles.

The only systematic direct measurements of mass flux profiles in the east Pacific are from velocity-azimuth display (VAD) analyses of Doppler radar data (Mapes and Lin, 2005) from the ship *Ronald H. Brown* during the EPIC2001 program, and the earlier Tropical Eastern Pacific Process Study (TEPPS; Yuter and Houze, 2000). During EPIC2001, observations were made at 95 W, 10 N, while TEPPS observations were located primarily at 125 W, 8 N. The divergence profiles from EPIC2001 observations suggest rather top-heavy mass flux profiles, with those from TEPPS being somewhat less top-heavy. However, these observations give no hint as to the latitudinal structure of vertical mass flux profiles and are somewhat biased toward highly disturbed situations, as VAD techniques require good reflective cloud coverage in the vicinity of the radar in order to work.

Some additional profiles were derived from airborne Doppler radar measurements in developing tropical cyclones during the 1991 Tropical Experiment in Mexico (TEXMEX; Bister and Emanuel, 1997; Raymond et al., 1998). These tended to show top-heavy mass flux profiles early in the formation stage, evolving toward bottom-heavy profiles as the cyclones intensified. However, these measurements were sporadic and generally located to the north of the climatological ITCZ, as were the EPIC2001 measurements.

Convection and Easterly Waves

A vast literature exists on easterly waves, which cannot be reviewed in detail here. The most important points are as follows:

1. Dynamically, these disturbances are vorticity anomalies with maximum vorticity in the lower (central and west Pacific; Reed and Recker, 1971; Tai and Ogura, 1987) or mid-troposphere (eastern Atlantic, east Pacific; Kiladis et al., 2006; Raymond et al., 1998) and tend to be close to geostrophic balance (Cho and Jenkins, 1987).

2. Jenkins and Cho (1991) showed that these disturbances evolve as described by the vorticity equation, with vertical stretching being the dominant mechanism by which convection modifies the vorticity (see also Rydbeck and Maloney, 2015). Raymond et al. (2015) advance a similar hypothesis.

3. Like tropical waves in many regions, east Pacific easterly wave troughs are oriented NE-southwest, resulting in conversion of zonal to eddy kinetic energy when zonal easterlies increase with latitude (Molinari et al., 1997; Maloney and Hartmann, 2001; Hartmann and Maloney, 2001; Petersen et al., 2003; Serra et al., 2010; Rybeck and Maloney, 2014, 2015).

4. The vertical structure is rather variable, but the heaviest precipitation tends to be located where the upper troposphere is warmer and the lower troposphere is cooler than the surrounding environment. This often occurs on or east of the trough (Peterson et al., 2003; Serra et al., 2010). Such a temperature dipole is associated with low instability index, which agrees with the above results correlating bottom-heavy vertical mass fluxes and stronger precipitation with lower values of this parameter.

The origin of east Pacific easterly waves is uncertain. At least some waves are simply African waves that cross Central America into the east Pacific. However, strong wave genesis or intensification exists near $85 - 90$ W, $8 - 10$ N (Serra et al., 2010; Rydbeck and Maloney, 2014, 2015). Zehnder (1991), Mozer and Zehnder (1996) and Farfán and Zehnder (1997) proposed that easterly waves and tropical cyclones can form as a result of lee forcing by the mountains of Central America. This forcing results in the formation of an easterly coastal jet along the Pacific coast, which interacts with the ITCZ and a jet through the Isthmus of Tehuantepec to produce a closed cyclonic circulation at low levels. Local barotropic instability may also create or intensify waves, as noted above.

In contrast, Kerns et al. (2008) found that many of the positive vorticity anomalies in the layers $850 - 925$ hPa and $600 - 700$ hPa originate south of Central America, just off the Pacific coasts of Colombia and Panama in the $5 - 10$ N latitude range. Most the vorticity anomalies that intensify into tropical storms appear to come from this region according to their analysis. Rydbeck and Maloney (2015) find similar results. Thus, significant uncertainty remains as to the origin of east Pacific easterly waves.

The far eastern part of the cross-equatorial boundary layer flow in the east Pacific turns to the east and impinges on the coast of Colombia. This flow is locally called the Chocó jet. Its collision with the westernmost cordillera of the Andes produces what are arguably the largest annual rainfalls in the world, up to 13 m yr^{-1} (Poveda and Mesa, 2000). TRMM precipitation radar measurements show that this heavy rainfall extends well offshore into the heart of the Chocó jet (Zulaga and Houze, 2015). This area of heavy rain coincides with strong production of east Pacific vorticity anomalies (Kerns et al., 2008). We hypothesize that the convection in the Chocó jet is in fact responsible for producing at least some of this vorticity. The Chocó jet is one of the regions exhibiting weak cellular convection according to Zuluaga and Houze (2015) and Houze et al. (2015). A study of this region could therefore help resolve two outstanding questions, the nature of this type of convection and the origin of at least some east Pacific easterly waves.

Easterly waves are a reliable feature of the summertime east Pacific, appearing every 6 d or so. Occasionally, eastward-moving equatorial Kelvin waves penetrate to the east Pacific (e.g., Straub and Kiladis, 2002). As these disturbances are essentially unbalanced, their appearance in the east Pacific would provide an opportunity to study a different type of convective interaction. In addition, active and passive phases of the Madden-Julian oscillation (MJO) or some close analog act on the east Pacific. The primary effect of the MJO is to modify the environment in which easterly waves and tropical cyclones occur (Maloney and Hartmann, 2000, 2001; Hartmann and Maloney, 2001; Raymond et al., 2006; Rydbeck and Maloney, 2014, 2015). The action of the MJO (if it materializes during our observational period) would therefore be documented by our observations of easterly waves.

A regular phenomenon called the "midsummer drought" occurs in the east Pacific (Amador et al., 2006; Romero-Centeno et al., 2007). A change in the global circulation patterns results in a shift of convection southward away from the Mexican and Central American coast in July and early August and is associated with an increase in low-level easterlies. The effect on easterly waves would appear to be similar to that of the inactive phase of the MJO.

Diurnal Cycle

Ocean locations remote from land experience a precipitation maximum near $0300 - 0400$ hr local time and an infrared brightness temperature minimum near 0600 hr. However, the diurnal cycle in the east Pacific is a result of both local radiative effects typical of remote ocean areas and of gravity waves emanating from convection over nearby land (Yang and Slingo, 2001; Mapes et al.,

2003a,b; Warner et al., 2003).

Using NOAA OLR precipitation estimates, Mapes et al. (2003a) found that convection in the Chocó jet offshore from the Colombian coast is sensitive to a diurnal wave propagating off the land, with maximum precipitation (during July, August, and September 2000) over the ocean between 0600 and 1000 hr local time. The estimate by Yang and Slingo (2001) is somewhat later, between 1000 and 1200 hr, whereas the numerical simulations of Warner et al. (2003) show precipitation forming along the coastal region somewhat earlier. In any case, these results are significantly different from the value of 0300 hr for the open ocean.

During EPIC2001, ship-borne radar near 95 W, 10 N showed a broad maximum in precipitation in the interval $0400 - 0700$ hr local time and a maximum in high-level cloudiness (and hence minimum OLR) near 0900 hr, while Yang and Slingo (2001) indicate maximum summertime rain near 1000 hr and minimum OLR near 1400 hr.

These results suggest that the Yang and Slingo (2001) precipitation maxima are biased $2 - 4$ hr late compared to model and observational results. However, taking this bias into account but assuming that the overall pattern is correct, their results suggest that most of the east Pacific ITCZ east of 110 W has a precipitation maximum in the range $0600 - 1100$ hr local time. Somewhat earlier maxima occur nearer the coasts of Central and South America.

OTREC: Organization of Tropical East Pacific Convection; Research Plan

Given the above discussion, the following scientific questions suggest themselves:

1. What are the factors that control the formation of deep convection in the tropical east Pacific and the southwest Caribbean, two very different regimes?

2. What form does convection take in these regions? In particular how do the vertical mass flux profile, thermodynamic budgets, and the value of the gross moist stability vary as a function of environmental conditions?

3. How do the interactions of convection with tropical disturbances work there, especially with tropical easterly waves?

Observational tools developed in the last decade, the use of which was perfected in recent field programs, can address the above questions in the tropical east Pacific and the southwest Caribbean.

Tools

Gulfstream V: In order to address the goals expressed above, we need to measure mesoscale vertical mass flux profiles, moisture and entropy budgets, the gross moist stability, and the mesoscale aggregate vorticity budget of convection in various locations in the east Pacific and southwest Caribbean. Dropsondes are the only realistic way of measuring these quantities. As these sondes need to be deployed from as high an altitude as possible, the aircraft of choice is the NSF/NCAR Gulfstream V (GV). Our group has well developed software tools for handling these measurements. We also have extensive operational experience in designing and implementing aircraft missions of this type.

In addition, we need to measure the radar reflectivity and vertical velocity structure of convection. We are especially interested in assessing cloud top height, particle vertical velocity spectra, and the presence or absence of bright bands. The Hiaper Cloud Radar (HCR) is the ideal radar for making the convective reflectivity and vertical velocity measurements in shallow and growing convection and in the upper parts of deep convection. This radar is housed in a pod that mounts
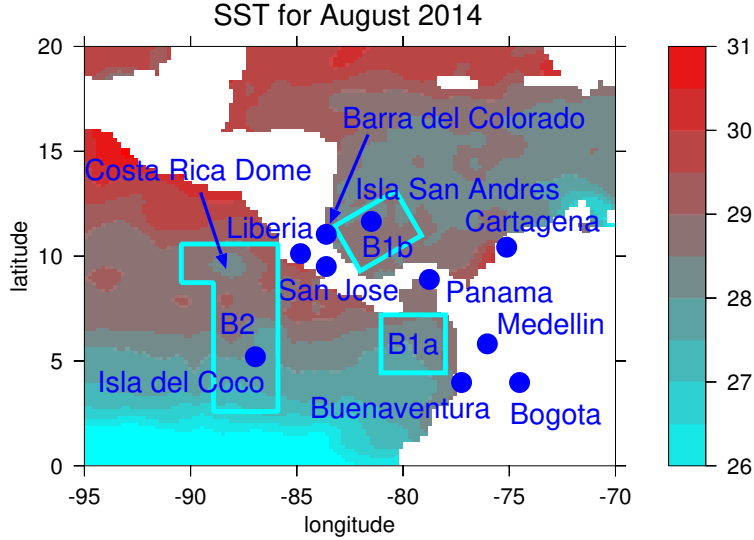
Figure 6: Overview of proposed operating regions for the G-V aircraft on a background of SST in August 2014. Boxes B1a and B1b would be flown on the same mission. The Costa Rica Dome is a semi-permanent region of ocean upwelling and lower SSTs near $90\,W, 9\,N$ (Wyrtki, 1964).

under the wing of the GV. Though the radar has some scanning capability, we would plan to operate it in vertically pointing mode in order to not contaminate the Doppler velocity measurements with horizontal winds. The HCR is a W-band radar (3.2 mm wavelength), which means that it is strongly attenuated by heavy precipitation. However, this is not a problem for studying raining shallow convection, as recent results from the CSET (Cloud Systems Evolution in the Trades; see https://www.eol.ucar.edu/field_projects/cset) project have demonstrated. In results we have seen from this radar for deep convection, the convective cores are highly attenuated, especially below the freezing level. However, the radar is able to penetrate stratiform clouds from above well enough to see the underlying bright bands, though their appearance at 94 GHz is more of a sharp discontinuity in reflectivity than a high reflectivity band at the freezing level (Kollias and Albrecht, 2005; Kollias et al., 2007). We are developing a plan to deal with the multiple terabytes of data produced by HCR.

Barra del Colorado Radiosonde: We propose to install a portable radiosonde station at Barra del Colorado Wild Life Refuge in NE Costa Rica near the Caribbean coast (84 W, 11 N). This location was suggested by Jorge Amador. Among other things, the radiosonde record would provide time continuity in Caribbean jet strength as well as early warning of easterly waves entering the east Pacific from the Caribbean. The New Mexico Tech physics department owns a portable radiosonde receiver that we can borrow, leaving only expendables to be purchased.

GPS Precipitable Water: COCONet (http://coconet.unavco.org/) is an array of GPS precipitable water instruments (Duan et al., 1996) in Central and Northern South America and the Caribbean. These instruments easily detect passing easterly waves (Yolande Serra, personal communication), which gives us a powerful tool in real time for flight planning purposes. GPS measurements would also provide context for analysis of the aircraft data.

Sea Surface Temperature: SST is needed for the computation of surface heat and moisture fluxes. The default product for this is the Optimum Interpolation SST (OISST; Reynolds et al., 2007; https://www.ncdc.noaa.gov/oisst), which provides daily SST maps on a 0.25 deg global grid. Other products based on passive microwave measurements are also available.

Satellite, Radiosondes, Radar, and Model Diagnostics: We will need to know in real time the location and strength of easterly waves and other disturbances. In addition to the Barra del Colorado sounding and the GPS precipitable water array, geosynchronous satellite loops (available online from the National Hurricane Center) and global model analyses and predictions will be used for this purpose. The Government of Colombia has dual polarization C-band radars installed in Bogotá, Cartagena, and Isla San Andrés and has plans to install another in Buenaventura. Real time displays for these radars exist online. We are investigating as to whether the data are recorded and whether they are available for research purposes. Medellín has a similar radar on a ridge overlooking the city. The data from this radar are freely available. Isla San Andrés and Bogotá also have radiosonde sites run by the Colombian Government.

Oxygen Isotope Ratios: Zhiming Kuang has proposed making oxygen isotope measurements in rainwater, as these ratios should give a long-term average indication of the "top-heaviness" of the convection. The idea is that top heavy convection draws in moist air from a deep layer, unlike bottom heavy convection. Since the isotope ratio is a sensitive function of height in the environment, these situations can be distinguished. Sampling sites in regions receiving oceanic ITCZ rainfall would be sought. Two possible sites would be Isla del Coco, Costa Rica and Buenaventura, Colombia. (See figure 6.) Nearby land sites (e.g., Medellín, Cartagena) could be used to provide comparsions with rain from vigorous deep convection.

GPM satellite: The Global Precipitation Measurement (GPM; http://www.nasa.gov/mission_pages/GPM/main/) satellite is a successor to the Tropical Rainfall Measuring Mission (TRMM; see Houze et al., 2015) satellite. OTREC would provide ground-truth measurements for testing rainfall algorithms that use GPM (or TRMM) data in the east Pacific. Coordinating aircraft and satellite measurements so as to target particular convective events at the same time is very difficult, so regional statistical comparisons are likely to be more fruitful.

Models: We plan to make extensive use of existing global models (e.g., those from NCEP and ECMWF), with possible special runs from the latter. Results from regional models (e.g., WRF) can also be tested for their ability to reproduce observational results. Cloud resolving models with weak temperature gradient parameterizations of the large scale (Shaevitz and Sobel, 2004; Raymond and Zeng, 2005; Raymond and Sessions, 2007; Sessions et al., 2010; Wang et al., 2013; Herman and Raymond, 2014; Sessions et al., 2015; Sentić et al., 2015) would be tested to see if they can reproduce the characteristics of east Pacific and southwest Caribbean convection, given the environmental conditions there. Finally, cloud resolving modeling would be used to make sense out of oxygen isotope measurements and to better understand the transition from shallow to deep convection.

Tactical Considerations

Flight operations are proposed for an eight week period in the summer of 2018 with a base in either San José or Liberia in Costa Rica (see figure 6). Any time between 1 June and 1 October for this

Cost element	Cost
GV Core (Gulfstream V 160 hr)	$1,506,421
AVAPS (600 dropsondes)	$606,024
HCR (cloud radar)	$239,986
CDS (data services)	$108,948
PMO/CWIG (operations center)	$297,551
Total	$2,758,930

Table 1: Cost estimate for the Gulfstream V operation as provided by NCAR/EOL.

eight week interval would be satisfactory, though later would be better for the Chocó jet, which peaks in September (Germán Poveda, personal communication).

Table 1 shows the cost estimate from NCAR/EOL to operate the GV with the specified instruments for 160 hr of flight time over the 8 week period. Approximately 20 flights of 8 hr each would be made, with 30 dropsondes expended per flight, resulting in 600 dropsondes. Flights would occur on the same daily schedule in order to eliminate the effect of the diurnal cycle, thus reducing the size of the parameter space to be explored.

Figure 6 shows the proposed operational areas for the GV. Box B1a covers the Chocó jet while B1b includes the normal area of transition to deep convection in the southwest Caribbean. Box B2 spans the ITCZ farther west, extending from the area of shallow convection on the south through the northern region of deep convection. The longitude of B2 is set to encompass the region of easterly wave genesis near 89 W, 10 N discussed earlier. The westward extension at the north end is designed to allow coverage of both the Costa Rica Dome and the adjacent warmer water. Easterly waves passing through B1a or B1b reach B2 about one day later, allowing flights on successive days to study the same westward-moving disturbance.

The two boxes B1a and B1b can be covered in the same flight. "Lawnmower" patterns would be used to deploy dropsondes on a $1 - 1.5$ deg grid that fills the specified boxes, much as was done in TPARC/TCS08 and in PREDICT. This provides ideal input for our three-dimensional variational scheme (López and Raymond, 2011). It would be desirable to deploy dropsondes in the gap between B1a and B1b, but this may not be operationally feasible, given the presence of the busy Panamá airport.

Building on lessons learned in EPIC2001, the same two-flight pattern, B1a and B1b on the first day and B2 on the second day, will be repeated without significant changes over the entire project period. This repetition allows stable composites of noisy convective processes to be constructed.

The positioning of the boxes in figure 6 assumes a non-El Niño year. In the unlikely event that an El Niño occurs in 2018, east Pacific SST gradients would be weaker and the north-south position of B2 would be adjusted accordingly. A weaker Chocó jet could also be expected. Slight repositioning of B2 in response to the position of the cool anomaly of the Costa Rica Dome would also be considered.

GPS precipitable water, radiosonde data, satellite observations, and global model analysis products and predictions will be used to determine the state of the atmosphere and the present and future location of easterly waves for flight planning purposes.

Measurement Goals

We have several goals for the observational phase of the program. These mainly involve using the dropsonde and cloud radar capabilities of the GV.

1. The dependence of mesoscale mass flux profiles, thermodynamic budgets, values of gross moist stability, and vorticity budgets on environmental conditions would be determined in all regions as a function of location and easterly wave phase using dropsonde arrays. Note that we are not mapping entire easterly waves; they are too big.

2. The cloud radar would be used to measure vertical hydrometeor velocity spectra and reflectivities in shallow and growing convection, deep convection above the freezing level, as well as regions with bright bands.

3. The possible evolution of convective characteristics within easterly waves will be examined by making measurements in B1a and B1b on one day and in B2 on the following day.

4. Oxygen isotope ratios in rain water will be measured to determine whether there is a signal that indicates the degree of top-heaviness of deep convection.

5. In addition to their operational function, GPS precipitable water measurements will be used to assess the character of convection during easterly wave passages across Central America.

Outreach

We have made contact with researchers at the Universidad Nacional de Colombia in Bogotá (Daniel Hernández) and the Universidad Nacional Facultad de Minas in Medellín (Germán Poveda, Oscar Mesa, Manuel Zuluaga), as well as Carlos Hoyos of the Sistema de Alerta Temprana de Medellín y el Valle de Aburrá. Manuel Zuluaga worked with Bob Houze on the latest revision to the TRMM precipitation algorithm, and his participation would be particularly valuable for that reason. The project was well received by the individuals contacted and we seek collaborations with Colombian investigators. Jorge Amador of the University of Costa Rica has been a part of the OTREC scientific team from the beginning.

Broader Impacts of the Proposed Work

1. Resolution of the uncertainty in vertical mass flux profiles of east Pacific convection including the Chocó jet has major implications for the proper diagnosis of convection from satellite observations, particularly those made by the new Global Precipitation Measurement satellite. This is also important for developing reliable convective parameterizations for global models. Our results would be obtained in the east Pacific and southwest Caribbean, but would be applicable to many other regions of the tropics.

2. Determination of the mechanisms controlling convection in regions with strong SST gradients would have broad applicability for the same reasons as discussed above. To the extent that the intensification of easterly waves becomes better understood, tropical cyclone forecasts would improve.

3. Execution of this project will require close cooperation with investigators from Costa Rica, Colombia, and possibly Panamá. Success in this regard would strengthen links between the atmospheric science communities in these countries and in the US.

4. One of the goals of this project will be to introduce young investigators, including students, into the arts of making airborne observations and running field programs. This experience can give young scientists the motivation and self confidence to initiate observational programs in their own right.